Modelling Low Charge Ions in the Solar Atmosphere

Roger Dufresne and Giulio Del Zanna

(DAMTP, University of Cambridge)

Nigel Badnell

(Department of Physics, University of Strathclyde)

Pete Storey

(University College London)

MNRAS 2020, 497, 1443; MNRAS 2021a, 503, 1976; MNRAS 2021b, 505, 3968

Background

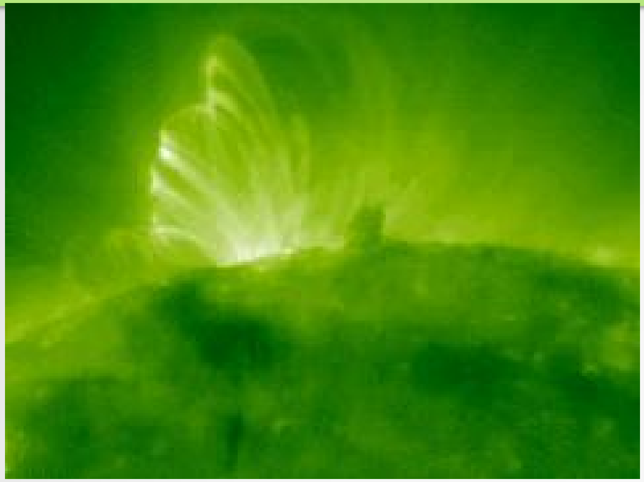

<u>Corona</u> ($6x10^5$-$3x10^6$ K) – steady state equilibrium, independent atom models, ground level ionisation and recombination

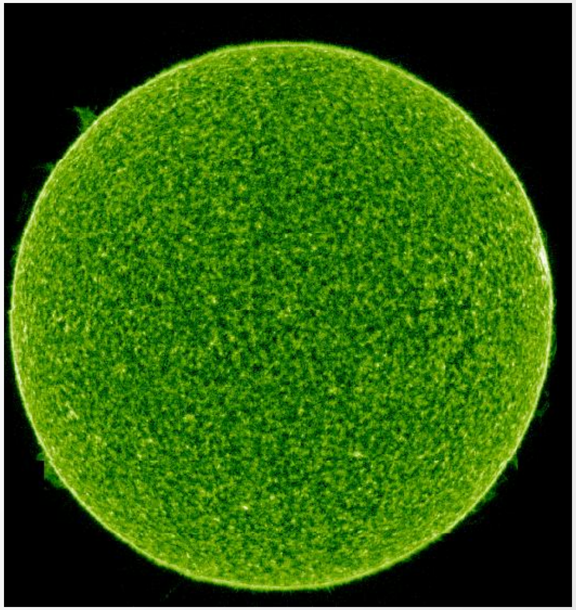

<u>Transition region</u> (25000-$6x10^5$K) - ?

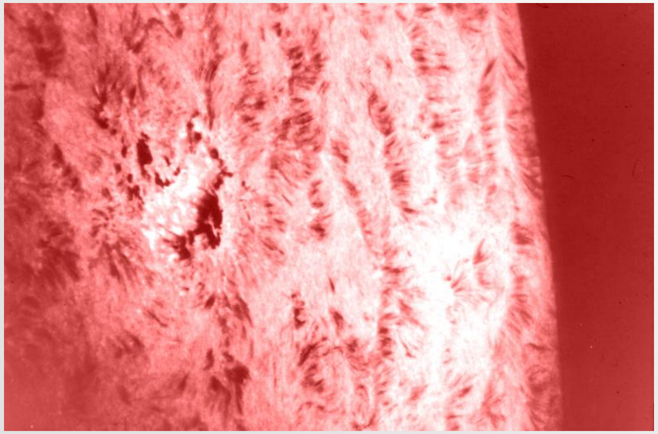

<u>Chromosphere</u> (6000-25000K)– Time-dependent ionisation, radiation hydrodynamics, photo-induced processes, charge transfer, inelastic collisions with hydrogen.

Modelling: Level Resolved

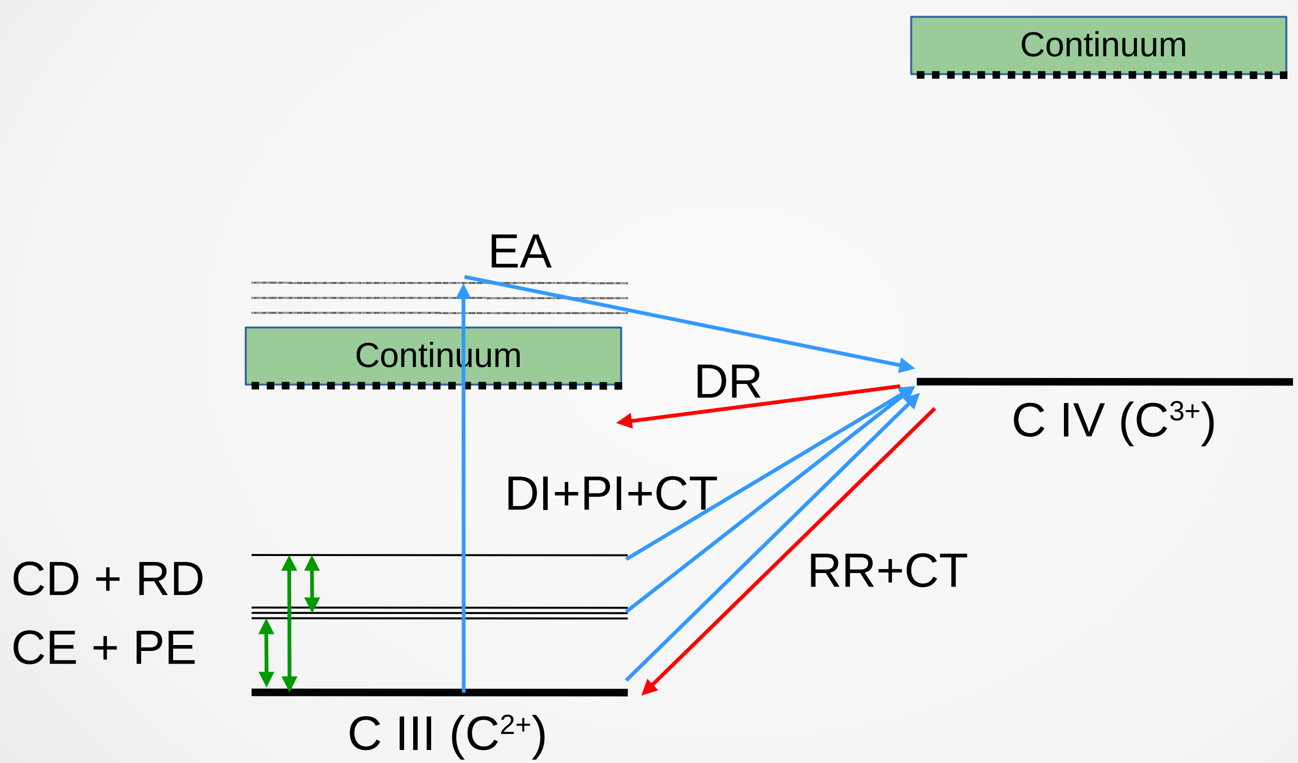

DI – Direct Ionisation PI – Photo-ionisation EA – Excitation-Autoionisation
RR/RD – Radiative Recombination/Decay DR – Dielectronic Recombination CT – Charge Transfer
CE/CD – Collisional Excitation/De-excitation PE – Photo-excitation

Methods: Modelling new atomic processes

Density effects

Ionisation and recombination from metastable levels:

- New ionisation rate calculations for carbon and oxygen, using Flexible Atomic Code (Gu, 2008, Can. J. Phys.,86, 675) and Autostructure (Badnell 2011, CPC, 182, 1528)
- Recombination data from APAP Network (Badnell 2006, ApJS, 167, 334, Badnell et al, 2003, A&A, 406, 1151)

Suppression of dielectronic recombination:

- Estimated from data of Summers, 1974, MNRAS, 169, 663.

Photo-ionisation

$$\alpha_{ij}^{PI} = 4\pi \int_{\nu_0}^{\infty} \frac{\sigma_{ij}(\nu)}{h\nu} \, J_\nu \, \mathrm{d}\nu$$

Cross sections from Badnell N. R., 2006, ApJS, 167, 334.
Radiances from Woods T. N., et al., 2009, Geophys. Res. Lett., 36, L01101.

Charge transfer

Reactions of type:
$A^{+z} + H \leftrightarrow A^{+(z-1)} + H^{+}$

$$R_{\mathrm{CT}}(T_{\mathrm{e}}) = \frac{N_{\mathrm{H\,I}}}{N_{\mathrm{H}}} \frac{N_{\mathrm{H}}}{N_{\mathrm{e}}} N_{\mathrm{e}} \, \alpha_{\mathrm{CT}}(T_{\mathrm{e}})$$

Hydrogen fractional populations taken from Avrett E. H., Loeser R., 2008, ApJS, 175, 229

Results: Ion Populations

With photo-ionisation only | With charge transfer only

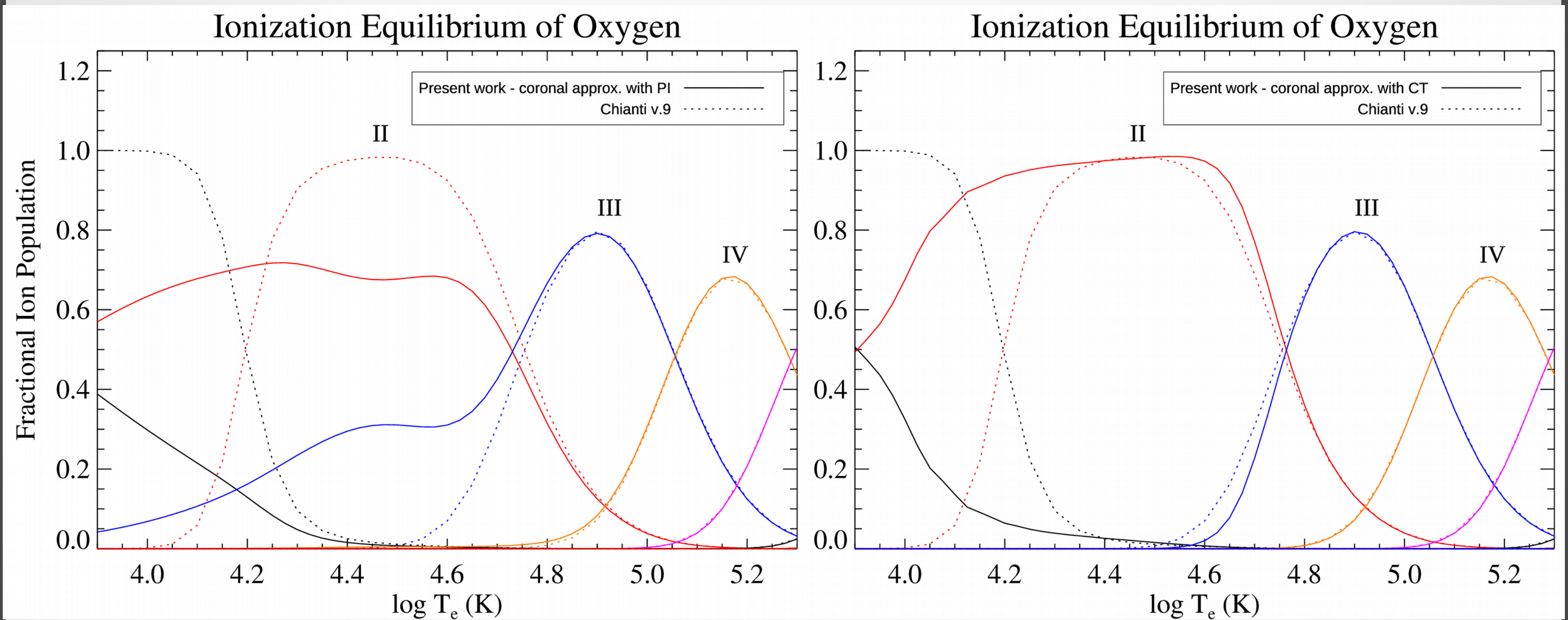

- O I depleted by both processes
- O II enhanced at low temperature
- Charge transfer opposes photo-ionisation of O II at higher temperature

Charge transfer data:
Stancil P. C., et al. 1999A, J. Phys. B, 32, 1523
Barragán P., et al. 2006, ApJ, 636, 544
Wang J. G., et al. 2003, Phys. Rev. A, 67, 012710
Wu Y., et al. 2009, Phys. Rev. A, 79, 062711

Results: Ion Populations

With all atomic processes combined

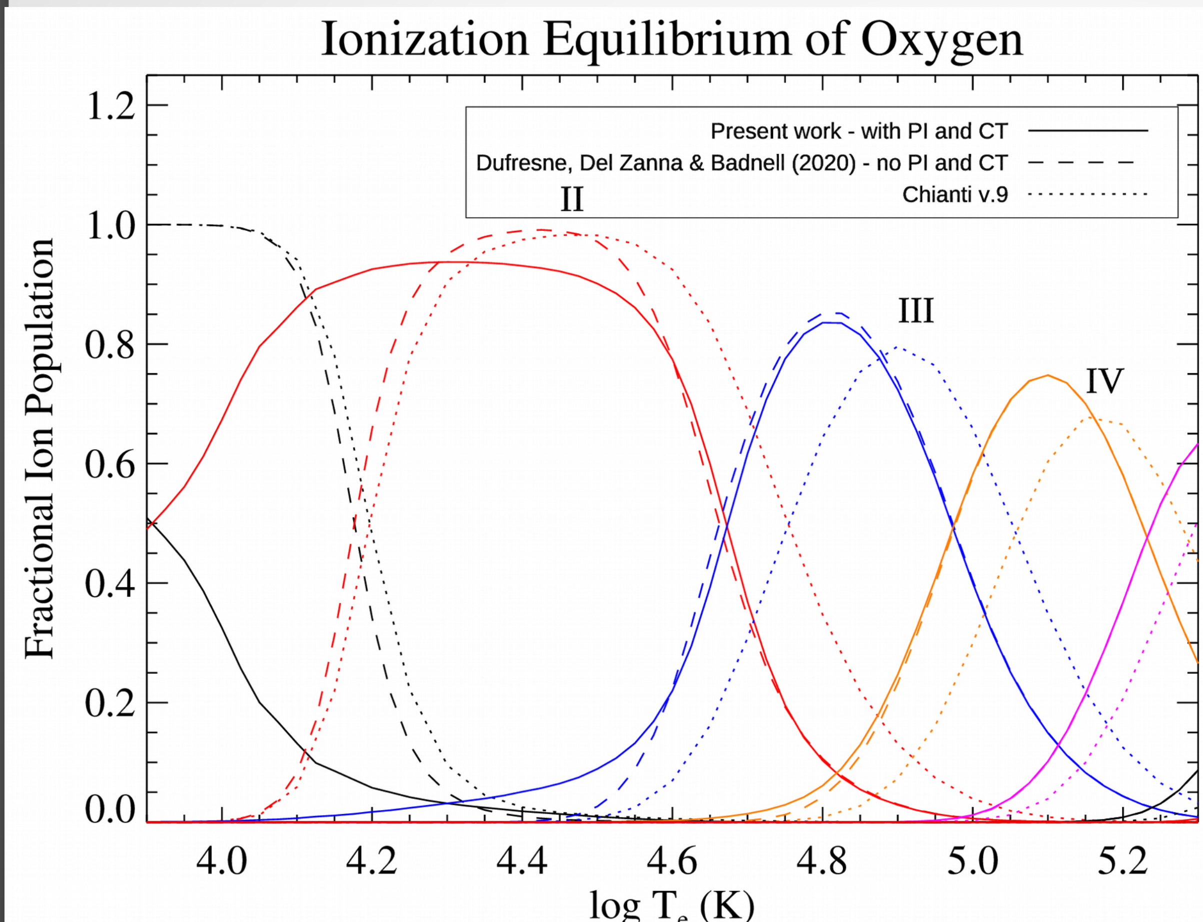

- Higher temperature O II lines and O III lines now agree with observations

Comparison with observations

Ion	λ_{obs}	I_{obs}	R_{c}	R_{e}	R_{f}
O II	832.75	11.2[a]	3.02	2.66	2.20
O II	834.45	35.5[a]	2.85	2.51	2.08
O II	833.32	24.5[a]	2.75	2.42	2.01
O II	718.49	15[a]	2.10	1.39	1.22
O II	796.66	2.84[d]	1.71	1.32	1.21
O III	1660.80	19.3[b]	0.44	0.61	0.79
O III	832.92	13.7[c]	1.21	1.32	1.37
O III	833.74	47.3[c]	1.06	1.14	1.19
O III	835.10	12.9[c]	0.98	1.06	1.10
O III	835.26	63.8[c]	1.09	1.19	1.23
O III	702.89	27.5[a]	1.16	1.15	1.17

Theoretical to observed intensities

R_c – coronal approximation

R_e – density effects added

R_f – charge transfer and photo-ionisation added

Results: Ion Populations

With all atomic processes combined

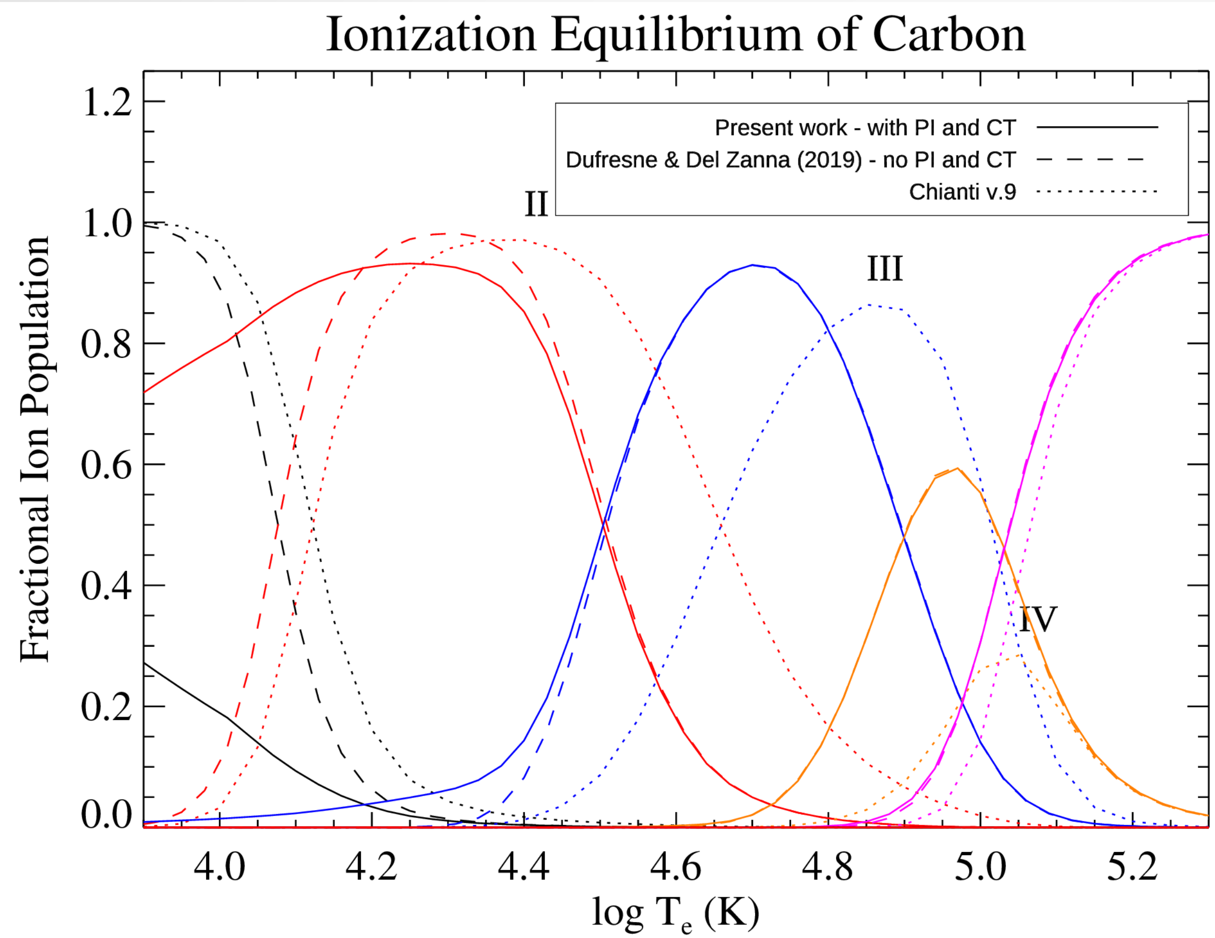

Comparison with observations

Ion	λ_{obs}	I_{obs}	R_c	R_e	R_f
C II	1334.53	937[a]	0.56	0.66	0.94
C II	1335.71	1350[a]	0.75	0.90	1.29
C II	1036.34	57.9[a]	0.92	0.81	0.69
C II	1037.00	70.1[a]	1.50	1.31	1.12
C II	903.99	9.98[a]	2.22	1.68	1.29
C II	904.46	6.29[a]	1.78	1.34	1.03
C II	903.59	9.19[a]	1.62	1.21	0.94
C II	904.14	23.1[a]	3.21	2.41	1.87
C II	1323.91	1.72[b]	2.47	1.30	0.98
C III	977.04	702[c]	0.65	0.86	0.87
C III	1174.88	37.4[c]	0.65	0.83	0.83
C III	1175.74	104[c]	0.71	0.89	0.89
C III	1176.37	36.2[c]	0.67	0.85	0.85
C IV	1548.24	212[b]	0.43	1.28	1.26
C IV	1550.82	134[b]	0.34	1.02	1.00

Theoretical to observed intensities

R_c – coronal approximation

R_e – density effects added

R_f – charge transfer and photo-ionisation added

- All predicted intensities in better agreement with observations

Results: Ion Populations

With all atomic processes combined

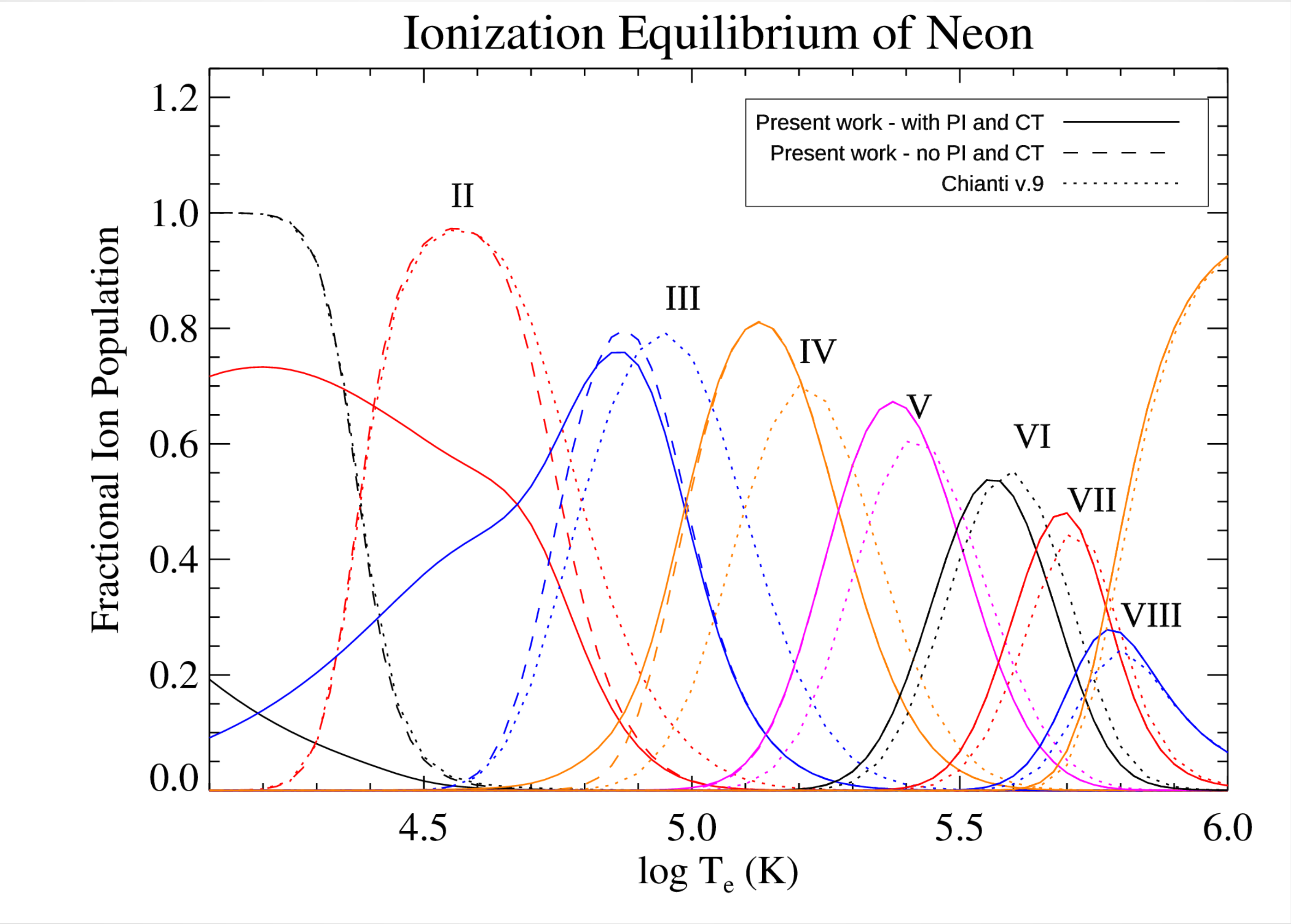

Results: Ion Populations

With all atomic processes combined

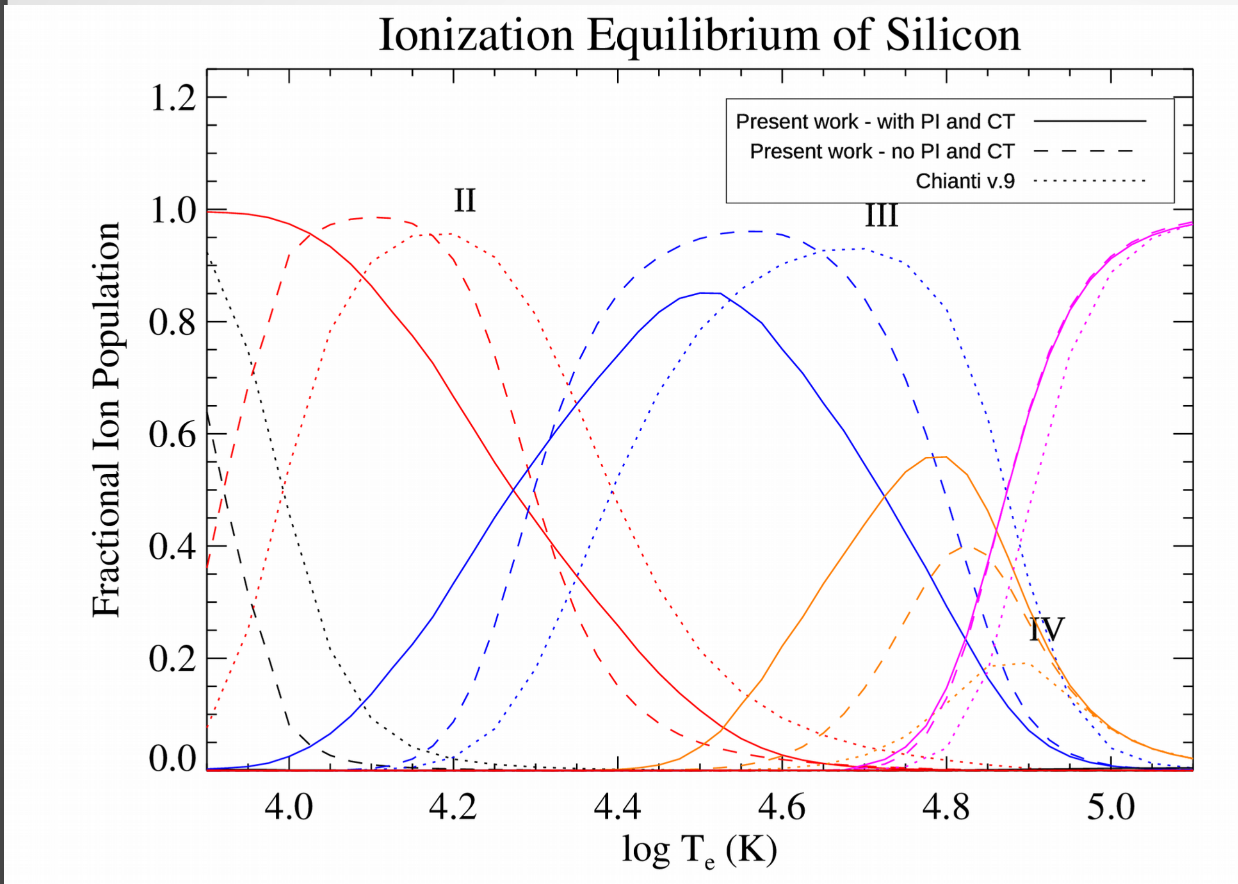

Comparison with observations

Ion	$\lambda_{\rm obs}$	$I_{\rm obs}$	$R_{\rm c}$	$R_{\rm e}$	$R_{\rm f}$
Si III	1892.03	832^h	0.47	0.85	1.08
Si III	1206.51	630^e	0.69	0.87	0.69
Si III	1294.54	4.9^e	0.84	0.84	0.60
Si III	1298.89	16.9^e	0.83	0.83	0.59
Si III	1296.73	3.8^e	0.83	0.84	0.60
Si III	1108.37	4.3^e	0.61	0.57	0.40
Si III	1109.97	6.5^e	1.00	0.92	0.66
Si III	1113.23	15.5^e	1.07	0.97	0.70
Si IV	1393.78	280^a	0.06	0.16	0.33
Si IV	1402.77	127^a	0.07	0.18	0.37

Theoretical to observed intensities

R_c – coronal approximation

R_e – density effects added

R_f – charge transfer and photo-ionisation added

- Predicted intensities of Si IV resonance lines increase by more than a factor of 5

CT data: Kimura M., et al. 1996, ApJ, 473, 1114
Clarke N., et al. 1999 J.Phys., 31, 533
Wang J. G., et al. 2006, Phys. Rev. A, 74, 052709
Stancil P. C., et al. 1999, J. Phys. B, 32, 1523

Modelling Ion Populations

Summary

1) Calculated level-resolved direct and indirect ionization rates
2) Metastable levels included in modelling
3) Simulated dielectronic recombination suppression in modelling
4) Added photo-induced and charge transfer processes
5) Improved predicted line intensities compared to observations

Future work

1) Find changes in diagnostics from new modelling
2) Add simplified optical depth effects for low temperature lines
3) Non-Maxwellian electrons
4) Time dependent ionisation

Results: Ion Populations

With all atomic processes combined